Proceedings Paper:

Teng, L., Wang, Q., Chen, H. et al. (3 more authors) (2020) DOA estimation for coexistence of circular and non-circular signals based on atomic norm minimization. In: 2020 IEEE 11th Sensor Array and Multichannel Signal Processing Workshop (SAM). 2020 IEEE 11th Sensor Array and Multichannel Signal Processing Workshop (SAM), 08-11 Jun 2020, Hangzhou, China. IEEE . ISBN 9781728119472

https://doi.org/10.1109/sam48682.2020.9104368

DOA Estimation for Coexistence of Circular and Non-Circular Signals Based on Atomic Norm Minimization

Liping Teng†, Qing Wang†, Hua Chen‡*, Wei-Ping Zhu§, Wei Liu¶, and Jingjing Cai‖
†Schcol of Electrical and Information Engineering, Tianjin University, Tianjin, 300072, China.
‡Key Laboratory of Intelligent Perception and Advanced Control of State Ethnic Affairs Commission, Dalian, 116600, China.
§Department of Electrical and Computer Engineering, Concordia University, Montreal, QC H3G 1M8, Canada.
¶Department of Electronic and Electrical Engineering, University of Sheffield, Sheffield, S1 3JD, United Kingdom.
‖Department of Electronic Engineering, Xidian University, Xian, 710071, China.

***Abstract*—In this paper, a gridless DOA estimation method with coexistence of non-circular and circular signals is proposed by employing an enhanced sparse nested array, whose virtual array has no holes. The virtual signals derived from both sum and difference co-arrays are constructed based on atomic norm minimization. Simulation results are provided to demonstrate the performance of the proposed method.**

***Index Terms*—DOA estimation, Enhanced nested sparse array, Virtual array, Atomic norm, Circular and non-circular signals**

I. Introduction

Direction-of-arrival (DOA) estimation is a key topic in array signal processing and plays an important role in radar, sonar, navigation, geophysics, acoustic tracking and many other applications [1]. In contrast to a uniform linear array, a sparse array can increase the array aperture and degrees of freedom (DOFs) through equivalent signals of the virtual array [2]. For instance, sparse array can identify up to $\mathcal{O}(N^2)$ sources with N physical sensors.

Nested array and coprime array are two well-studied sparse array structures, as their number of DOFs has a closed-form expression. The nested array proposed in [3] combined two uniform line arrays (ULAs) with increased sensors spacing, and the difference co-array of this nested array is uniform and has no holes. Since this specific nested array is susceptible to mutual coupling given its close sensor spacing, a new class of nested arrays was proposed in [4], which can increase DOFs and reduce mutual coupling, but their sum co-array has holes. In [5], the coprime array was proposed with reduced mutual coupling, however, its number of DOFs is smaller than nested arrays given the same number of sensors [6]. A generalized coprime array was presented in [7], which can increase DOFs and extend the consecutive part of the virtual array. Yet it is generally not attractive compared to the nested array and its virtual array also has holes. Recently, a sparse conventional nested array with uniform sum and difference co-arrays was constructed in [8], and it can provide a basis for further exploring the DOA estimation methods based on both sum and difference co-arrays.

Most of the methods assume either explicitly or implicitly that the source signals are circular. In [9] and [10], an ESPRIT-like joint diagonalization method was proposed with uniform arrays for a mixture of circular and strictly non-circular sources. In [11], a new data vector was constructed by combining the received uniform array data with its conjugate counterparts. In [12], a DOA estimation method was achieved by concatenating the original data and the conjugate ones; however, this method does not work when the directions of non-circular and circular sources are the same. In [13], acircularity difference-based method was proposed which can realize the estimation of the same DOA for mixed signals and is suitable for uniform arrays. In [14], polarization channel estimation was achieved for a mixture of circular and non-circular signals based on the unconjugated covariance matrix and covariance matrix differrencing, respectively.

Considering these two trends, the DOA estimation problem for a mixture of circular and non-circular signals employing sparse arrays is studied in this work, based on sparse signal represention (SSR). In SSR, since the array signal parameter space is continuous, the mesh of parameter space will cause the problem of base mismatch. To avoid this problem, some gridless methods have been proposed for DOA estimation. In [15], a low-rank matrix reconstruction (LRMR) method was developed with the rank norm replaced by the nuclear norm. A virtual array interpolation-based algorithm for coprime array DOA estimation was proposed in [16], where the atomic norm of the second-order virtual array signals was defined based on the interpolated virtual array.

In this paper, a DOA estimation method based on atomic norm is developed, which can still work when the sources are circular and non-circular signals. The sparse convolution array proposed in [8] is employed here for DOA estimation for the

This work is sponsored by the National Natural Science Foundation of China under Grant (No. 61871282, No. 61805189), the Key Laboratory of Intelligent Perception and Advanced Control of State Ethnic Affairs Commission under Grant MDIPAC-2019102, and by Zhejiang Provincial Natural Science Foundation of China under Grant (No. LQ19F010002).
*Corresponding author: Hua Chen, Email: dkchenhua0714@hotmail.com

first time, where the no-hole virtual difference and sum will be exploited.

Notations: $\otimes$, $||\cdot||_{\mathcal{A}}$ and $||\cdot||_F$ denotes the Kronecker product, atomic norm and frobenius norm, respectively. $(\cdot)^{\mathrm{H}}$, $(\cdot)^{\mathrm{T}}$ and $(\cdot)^*$ respectively stand for conjugate transpose, transpose and complex conjugation. The symbol $\mathrm{E}(\cdot)$ represents the statistical expectation, $diag(\cdot)$ denotes a diagonal matrix composed of the involved elements and $vec(\cdot)$ stands for the vectorization of a matix.

II. Signal Model and Problem Formulation

A. Signal Model

In this paper, a coexistence signal model is adopted, including both non-circular and circular signals. Consider a sparse array $\mathcal{S}$, consisting of N sensors spaced by d, with N being an integer and d being half wavelength, i.e $d=\lambda/2$. Assume there are K_{nc} non-circular and K_c circular narrow-band uncorrelated far field sources from directions $\theta=[\theta_{nc,1},\theta_{nc,2},\ldots,\theta_{nc,K_{nc}},\theta_{c,1},\theta_{c,2},\ldots,\theta_{c,K_c}]$. The source signals can be expressed in a vector form as

$$\mathbf{s}(t)=\left[\begin{array}{c}\mathbf{s}_{nc}(t)\\ \mathbf{s}_{c}(t)\end{array}\right] \tag{1}$$

where

$$\mathbf{s}_{nc}(t)=[s_{nc,1}(t),s_{nc,2}(t),\ldots s_{nc,K_{nc}}(t)]^{\mathrm{T}} \tag{2}$$

$$\mathbf{s}_{c}(t)=[s_{c,1}(t),s_{c,2}(t),\ldots s_{c,K_c}(t)]^{\mathrm{T}} \tag{3}$$

The signals received by the sparse array $\mathcal{S}$ can be expressed as

$$\mathbf{x}(t)=\mathbf{A}\mathbf{s}(t)+\mathbf{n}(t) \tag{4}$$

where, $\mathbf{n}(t)$ is the independent and identically distributed zero-mean additive white Gaussian noise vector, $\mathbf{n}(t)\sim\mathcal{CN}(\mathbf{0},p_n\mathbf{I})$ with p_n being the noise power and $\mathbf{I}$ the identity matrix, and $\mathbf{A}$ represents the array manifold matrix given by

$$\mathbf{A}=[\mathbf{A}_{nc},\mathbf{A}_{c}]\in C^{N\times K} \tag{5}$$

with

$$\mathbf{A}_{nc}=[\mathbf{a}(\theta_{nc,1}),\mathbf{a}(\theta_{nc,2}),\ldots\mathbf{a}(\theta_{nc,K})]\in C^{N\times K_{nc}} \tag{6}$$

$$\mathbf{A}_{c}=[\mathbf{a}(\theta_{c,1}),\mathbf{a}(\theta_{c,2}),\ldots\mathbf{a}(\theta_{c,K})]\in C^{N\times K_{c}} \tag{7}$$

where $\mathbf{a}(\theta_{c/nc,k})$ represents the steering vector of the kth source, $k\in[1,2,\ldots K]$, $K=K_{nc}+K_c$.

The covariance matrix of the recived signals is given by

$$\mathbf{R}_{\mathcal{S}}=\mathrm{E}[\mathbf{x}(t)\mathbf{x}^{\mathrm{H}}(t)]=\sum_{k=1}^{K}p_k\mathbf{a}(\theta_k)\mathbf{a}^{\mathrm{H}}(\theta_k)+p_n\mathbf{I} \tag{8}$$

where p_k is the power of source signals.

The pseudo covariance matrix of the recevived array signals is given by [17]

$$\mathbf{R}_{\mathcal{S}}^{'}=\mathrm{E}[\mathbf{x}(t)\mathbf{x}^{\mathrm{T}}(t)]=\sum_{k=1}^{K}\rho_k e^{j\varphi_k}p_k\mathbf{a}(\theta_k)\mathbf{a}^{\mathrm{T}}(\theta_k) \tag{9}$$

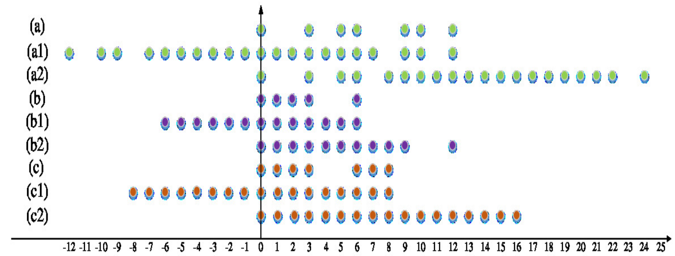

Fig. 1. Sparse array and virtual array construction. (a) Coprime array, M=3, N=5. (a1) Difference co-array of coprime array. (b) Sum co-array of coprime array. (b) Nested array, N1=3, N2=3. (b1) Difference co-array of nested array. (b2) Sum co-array of nested array. (c) ENested array, N=9, N1=3, N2=3. (c1) Difference co-array of ENested array. (c2) Sum co-array of ENested array.

where φ_k is the non-circularity phase and ρ_k is the non-circularity rate; for non-circular signals, $0<\rho_k\leq 1$ and for circular signals, $\rho_k=0$. Therefore, the pseudo covariance matrix has only the information of non-circular signals, and its corresponding elements are zero for circular signals. For the covariance matrix, the non-circular and circular signals are both non-zero [17].

In practice, the covariance and pseudo covariance matrices are normally replaced by their respective finite sample approximation as follows

$$\hat{\mathbf{R}}_{\mathcal{S}}=\frac{1}{L}\sum_{t=1}^{L}\mathbf{x}(t)\mathbf{x}^{\mathrm{H}}(t) \tag{10}$$

$$\hat{\mathbf{R}}_{\mathcal{S}}^{'}=\frac{1}{L}\sum_{t=1}^{L}\mathbf{x}(t)\mathbf{x}^{\mathrm{T}}(t) \tag{11}$$

where L is the number of snapshots.

B. Sparse Array Construction

The enhanced nested (ENested) array consists of the original nested array and an additional array [8]. N_1 and N_2 is the integer, $N=N_1*N_2$. The position set of the ENested array can be expressed as

$$\begin{aligned}\mathcal{S}_{ENested}=&\{n|n=0,1,\ldots\ldots N_1-1\}\\ &\cup\{nN_1|n=0,1,\ldots\ldots N_2-1\}\\ &\cup\{n|n=N-N_1,\ldots\ldots N-1\}\end{aligned} \tag{12}$$

Fig. 1(c) shows the ENested array with $N_1=3$ and $N_2=3$ $N=9$ as an example.

The coprime array [16] and nested array are shown in the Fig. 1(a) and Fig. 1(b). The difference and sum co-array of coprime array, nested array and ENested array are shown in the Fig. 1(a1) (a2), (b1) (b2) and (c1) (c2), respectively. Obviously, the sum and difference co-array of ENnested array have no holes as shown Fig. 1(c1) and Fig. 1(c2), and in this paper, we will further explore DOA estimation performance based on the ENnested array for the coexistence of circular and non-circular signals.

III. ENESTED ARRAY FOR DOA ESTIMATION

A. DOA Estimation for Non-circular Signals

For the pseudo covariance matrix in Eq. (9), due to the coexistence of circular and non-circular signals, we can further write it as

$$\mathbf{R}_{\mathcal{S}}^{'} = \mathbf{A}_{nc}\mathbf{R}_{nc}^{'}\mathbf{A}_{nc}^{\mathrm{T}} + \mathbf{A}_{c}\mathbf{R}_{c}^{'}\mathbf{A}_{c}^{\mathrm{T}} \tag{13}$$

where $\mathbf{R}_{nc}^{'} = \mathrm{E}[\mathbf{s}_{nc}\mathbf{s}_{nc}^{\mathrm{T}}]$ and $\mathbf{R}_{c}^{'} = \mathrm{E}[\mathbf{s}_{c}\mathbf{s}_{c}^{\mathrm{T}}]$. Since the non-circular ratio of the circular signal $\rho_k = 0$, $\mathbf{R}_{c}^{'} = 0$. Then Eq. (13) is simplified as

$$\mathbf{R}_{\mathcal{S}}^{'} = \mathbf{A}_{nc}\mathbf{R}_{nc}^{'}\mathbf{A}_{nc}^{\mathrm{T}} \tag{14}$$

The $\mathcal{U}_{sum}$ is defined as the distinct elements in the sum coarray position set $\tilde{\mathcal{U}}_{sum}$. The virtual vector of sum coarray can be obtained by vectorizing $\mathbf{R}_{\mathcal{S}}^{'}$ as

$$\mathbf{y}_{\tilde{\mathcal{U}}_{sum}} = vec(\mathbf{R}_{\mathcal{S}}^{'}) = \sum_{k=1}^{K_{nc}} \rho_k e^{j\varphi_k} p_k \mathbf{a'}_{nc}(\theta_k) \tag{15}$$

where

$$\mathbf{a'}_{nc}(\theta_k) = \mathbf{a}_{nc}(\theta_k) \otimes \mathbf{a}_{nc}(\theta_k) \tag{16}$$

The virtual array signals of sum coarray can be obtained from vector $\mathbf{y}_{\tilde{\mathcal{U}}_{sum}}$

$$\mathbf{y}_{\mathcal{U}_{sum}} = \sum_{k=1}^{K_{nc}} \rho_k p_k e^{j\varphi_k} \mathbf{v}_{nc}(\theta_k) \tag{17}$$

where $\mathbf{v}_{nc}(\theta_k)$ is the chosen equivalent steering vector from the $\mathbf{a'}_{nc}(\theta_k)$. The information in $\mathbf{a'}_{nc}(\theta_k)$ correspond to the elements in the $\tilde{\mathcal{U}}_{sum}$ array and the information in $\mathbf{v}_{nc}(\theta_k)$ correspond to the elements in the $\mathcal{U}_{sum}$ array.

Inspired by the atomic norm theory [18], [19], we absorb the non-circular phase φ_k and the $e^{j\varphi_k}$ into the following atomic set

$$\mathcal{A} = \{\mathbf{v}(\theta_k, \varphi_k)\,|\theta_k \in [0^\circ, 180^\circ], \varphi_k \in [0^\circ, 180^\circ]\} \tag{18}$$

The virtual measurements can be expressed in the form of atomic norm minimization as follows

$$\|\mathbf{y}_{\mathcal{U}_{sum}}\|_{\mathcal{A}} = \inf_{\rho_k, p_k} \left\{ \begin{array}{l} \sum\limits_{k}^{K_{nc}} \rho_k p_k : \\ \mathbf{y}_{\mathcal{U}_{sum}} = \sum\limits_{k=1}^{K_{nc}} \mathbf{v}(\theta_k, \varphi_k)\rho_k p_k, \\ p_k \geq 0, 0 < \rho_k \leq 1 \end{array} \right\} \tag{19}$$

Taking the error into account in the semi-definite programming (SDP) constraints [18], [19], the optimization problem can be expressed as

$$\begin{aligned} \min_{\mathcal{T},u} \frac{1}{2}u + \frac{1}{2N_{\mathcal{U}_{sum}}} Tr\left[\mathcal{T}'\right] + \frac{1}{2}\left\|\hat{\mathbf{y}}_{\mathcal{U}_{sum}} - \mathbf{y}_{\mathcal{U}_{sum}}\right\|_2^2 \\ s.t. \begin{bmatrix} u & \mathbf{y}_{\mathcal{U}_{sum}}^{\mathrm{H}}. \\ \mathbf{y} & \mathcal{T}' \end{bmatrix} \geq 0, \end{aligned} \tag{20}$$

where $\mathcal{T}'$ is a Hermitian Toeplitz matrix.

$$\mathcal{T}' = \sum_{k=1}^{K_{nc}} \rho_k p_k \mathbf{v}(\theta_k, \varphi_k)\mathbf{v}^{\mathrm{H}}(\theta_k, \varphi_k) \tag{21}$$

$N_{\mathcal{U}_{sum}}$ denotes the sensors numbers of sum co-array. If φ_k are all zero-valued, we have $\mathbf{v}(\theta_k, 0)$, leading to

$$\begin{aligned} \mathcal{T}' &= \sum_{k=1}^{K_{nc}} \rho_k p_k \mathbf{v}(\theta_k, \varphi_k)\mathbf{v}^{\mathrm{H}}(\theta_k, \varphi_k) \\ &= \sum_{k=1}^{K_{nc}} \rho_k p_k \mathbf{v}(\theta_k, 0)\mathbf{v}^{\mathrm{H}}(\theta_k, 0) \end{aligned} \tag{22}$$

According to Eq. (22), the $\mathcal{T}'$ corresponding to the atomic set containing θ_k and φ_k is equal to the $\mathcal{T}'$ corresponding to the atomic set only containing θ_k.

Eq. (20) is convex, we can solve the optimization problem by the CVX Tool box in MATLAB, the covariance matrix $\mathcal{T}'$ of sum virtual array is obtained by solving Eq. (20), and a MUSIC method can be used to estimate DOA $\theta_{nc,k}$ of non-circular signals.

B. DOA estimation for Circular Signals

For estimating DOA of circular sources, we need analyse the convariance matrix shown as Eq. (8), it can be expressed as

$$\mathbf{R}_{\mathcal{S}} = \mathbf{A}_{nc}\mathbf{R}_{nc}\mathbf{A}_{nc}^{\mathrm{H}} + \mathbf{A}_{c}\mathbf{R}_{c}\mathbf{A}_{c}^{\mathrm{H}} \tag{23}$$

where $\mathbf{R}_{nc} = E[\mathbf{s}_{nc}\mathbf{s}_{nc}^{\mathrm{H}}]$ and $\mathbf{R}_{c} = E[\mathbf{s}_{c}\mathbf{s}_{c}^{\mathrm{H}}]$.

Based on the DOAs of non-circular signals and Eq. (14), we can obtain $\mathbf{R}_{nc}^{'}$, and the $\mathbf{R}_{nc}$ can be expreseed as [13]

$$\mathbf{R}_{nc} = diag\{\left|R_{nc}^{'}(1,1)\right|, \ldots \left|R_{nc}^{'}(K_{nc}, K_{nc})\right|\} \tag{24}$$

Then, based on $\mathbf{R}_{nc}$, we can estimate the covariance matrix of non-circular signals. The covariance matrix of circular signals can be obtained by subtracting the covariance matrix of the non-circular part from Eq. (23) [13], giving

$$\mathbf{R} = \mathbf{R}_{\mathcal{S}} - \mathbf{A}_{nc}\mathbf{R}_{nc}\mathbf{A}_{nc}^{\mathrm{H}} \tag{25}$$

The difference virtual vector can be obtained by vectorizing $\mathbf{R}$ as

$$\mathbf{y}_{\tilde{\mathcal{U}}_{diff}} = vec(\mathbf{R}) = \sum_{k=1}^{K_c} p_k \mathbf{a'}_{c}(\theta_k) + p_n \mathbf{i} \tag{26}$$

where

$$\mathbf{a'}_{c}(\theta_k) = \mathbf{a}_{c}(\theta_k) \otimes \mathbf{a}_{c}^{*}(\theta_k) \tag{27}$$

The virtual signals of the difference co-array are obtained from vector $\mathbf{y}_{\tilde{\mathcal{U}}_{diff}}$ as

$$\mathbf{y}_{\mathcal{U}_{diff}} = \sum_{k=1}^{K_c} p_k \mathbf{z}(\theta_k) + p_n \bar{\mathbf{i}} \tag{28}$$

where $\mathbf{z}(\theta_k)$ is the obtained equivalent steering vector from the $\mathbf{a'}_{c}(\theta_k)$.

Based on the atomic norm theory, we have the the atomic set of difference coarray and virtual measurements as follows

$$\mathcal{A} = \{\mathbf{z}(\theta_k)\,|\theta_k \in [0^\circ, 180^\circ]\} \tag{29}$$

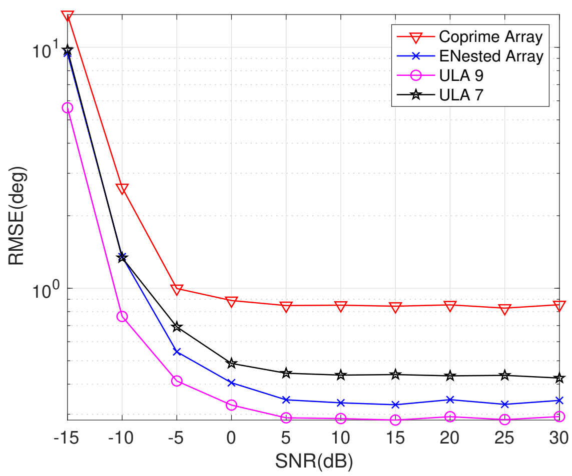

Fig. 2. RMSE versus the SNR.

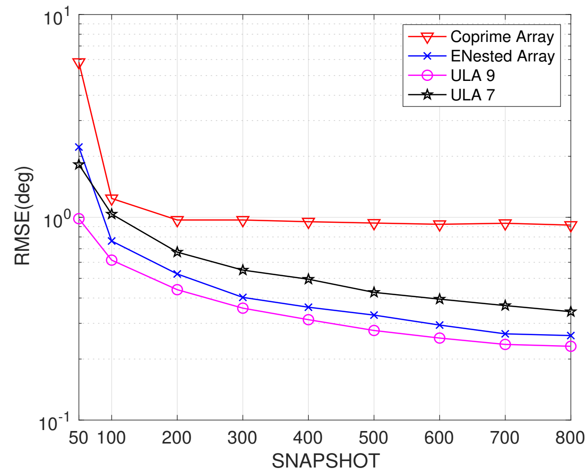

Fig. 3. RMSE versus the snapshot number.

$$\left\|\mathbf{y}_{\mathcal{U}_{diff}}\right\|_{\mathcal{A}} = \inf_{p_k}\left\{\sum_{k}^{K_c} p_k : \mathbf{y}_{\mathcal{U}_{diff}} = \sum_{k=1}^{K_c} \mathbf{z}(\theta_k) p_k, p_k \geq 0\right\} \tag{30}$$

Note that the equivalent SDP form of Eq. (30) is given by

$$\begin{aligned} &\min_{\mathcal{T},t} \frac{1}{2}t + \frac{1}{2N_{\mathcal{U}_{diff}}} Tr\left[\mathcal{T}\right] \\ &s.t. \left[\begin{array}{cc} t & \mathbf{y}^{\mathrm{H}}_{\mathcal{U}_{diff}} \\ \mathbf{y}_{\mathcal{U}_{diff}} & \mathcal{T} \end{array}\right] \geq 0 \end{aligned} \tag{31}$$

where $\mathcal{T}$ is a Hermitian Toeplitz matrix

$$\mathcal{T} = \sum_{k=1}^{K_c} p_k \mathbf{z}(\theta_k)\mathbf{z}^{\mathrm{H}}(\theta_k) \tag{32}$$

L denotes the sensor number of virtual array, and $N_{\mathcal{U}_{diff}}$ denotes the sensor numbers of the difference co-array or the sensor numbers of the difference co-array with holes.

Considering the error of virtual signals into account in the SDP constraints, the optimization problem can be finally expressed as

$$\begin{aligned} &\min_{\mathcal{T},t} \frac{1}{2}t + \frac{1}{2N_{\mathcal{U}_{diff}}} Tr\left[\mathcal{T}\right] + \frac{1}{2}\left\|\hat{\mathbf{y}}_{\mathcal{U}_{diff}} - \mathbf{y}_{\mathcal{U}_{diff}}\right\|_2^2 \\ &\qquad s.t. \left[\begin{array}{cc} t & \mathbf{y}^{\mathrm{H}}_{\mathcal{U}_{diff}} \\ \mathbf{y}_{\mathcal{U}_{diff}} & \mathcal{T} \end{array}\right] \geq 0, \end{aligned} \tag{33}$$

Using the CVX tool to solve the convex problem, we can obtain $\mathcal{T}$, and the covariance matrix of the difference coarray signals. Again the MUSIC method is used to estimate the DOA of the circular signals.

IV. Simulation Results

In the simulation, an Enested array with $N_1 = 3$ and $N_2 = 3$ is used, which has a total number of 7 physical sensors, with their locations shown in Fig. 1(c). The virtual arrays are shown as Fig. 1(c1) and Fig. 1(c2). As a comparison, the coprime array of $M = 3$ and $N = 5$, with 7 physical sensors, and the signals of non uniform sum and difference virtual arrays are obtained via interpolation [16]. Besides, two uniform linear arrays with 7 and 9 physical sensors respectively are also considered for comparison.

There are four non-circular uncorrelated sources uniformly distributed in $[40°, 100°]$, and four circular uncorrelated sources uniformly distributed in $[45°, 105°]$. We investigate the RMSE of DOA estimation for the ENested array, the coprime array, the seven-sensor ULA and the nine-sensor ULA. The snapshot number is $L = 500$. The result of 200 Monte Carlo trials is presented in Fig. 2. It is observed that the RMSE of the ENested array is close to the nine-sensor ULA and better than the seven-sensor ULA. This is because the sum and difference co-arrays of the ENested array have a virtual aperture of the same size as the nine-sensor ULA. Besides, the DOA estimation result of the coprime array is worse than other arrays due to existence of holes in its virtual array. The RMSE result versus the snapshot number from the four arrays is presented in Fig. 3, where the SNR is set as $30dB$.

V. Conclusion

In this paper, the DOA estimation problem with coexistence of circular and non-circular signals has been studied. By employing the recently proposed ENested array, whose sum and difference co-arrays have no holes, the proposed method reconstructs the covariance matrix of the virtual signals of the sum and difference co-arrays based on atomic norm minimization, respectively. As demonstrated by computer simulations, the proposed method can achieve a performance close to the ULA with a physical aperture that is the same as the difference and sum combined virtual aperture of the employed ENested array. This is because two arrays have same numbers virtual sensors.

REFERENCES

[1] X. Wu, W.-P. Zhu, and J. Yan, "A high-resolution doa estimation method with a family of nonconvex penalties," *IEEE Transactions on Vehicular Technology*, vol. 67, no. 6, pp. 4925–4938, June 2018.

[2] Q. Shen, W. Liu, W. Cui, S. Wu, Y. D. Zhang, and M. G. Amin, "Low-complexity direction-of-arrival estimation based on wideband co-prime arrays," *IEEE/ACM Transactions on Audio, Speech, and Language Processing*, vol. 23, no. 9, pp. 1445–1456, Sep. 2015.

[3] P. Pal and P. P. Vaidyanathan, "Nested arrays: A novel approach to array processing with enhanced degrees of freedom," *IEEE Transactions on Signal Processing*, vol. 58, no. 8, pp. 4167–4181, Aug 2010.

[4] Z. Zheng, W. Wang, Y. Kong, and Y. D. Zhang, "Misc array: A new sparse array design achieving increased degrees of freedom and reduced mutual coupling effect," *IEEE Transactions on Signal Processing*, vol. 67, no. 7, pp. 1728–1741, April 2019.

[5] P. P. Vaidyanathan and P. Pal, "Sparse sensing with co-prime samplers and arrays," *IEEE Transactions on Signal Processing*, vol. 59, no. 2, pp. 573–586, Feb 2011.

[6] Z. Zheng, W.-P. Wang, Y. Kong, and Y. D. Zhang, "Misc array: A new sparse array design achieving increased degrees of freedom and reduced mutual coupling effect," *IEEE Transactions on Signal Processing*, vol. 67, no. 7, pp. 1728–1741, April 2019.

[7] S. Qin, Y. D. Zhang, and M. G. Amin, "Generalized coprime array configurations for direction-of-arrival estimation," *IEEE Transactions on Signal Processing*, vol. 63, no. 6, pp. 1377–1390, March 2015.

[8] R. Cohen and Y. C. Eldar, "Sparse convolutional beamforming for ultrasound imaging," *IEEE Transactions on Ultrasonics, Ferroelectrics, and Frequency Control*, vol. 65, no. 12, pp. 2390–2406, Dec 2018.

[9] H. Chen, C. Hou, W. Zhu, W.-P. Liu, Y. Dong, and Q. Wang, "Joint diagonalization based 2d doa estimation for mixed circular and strictly noncircular sources," in *2017 IEEE Radar Conference (RadarConf)*, May 2017, pp. 0001–0005.

[10] H. Chen, C. Hou, W.-P. Zhu, W. Liu, Y.-Y. Dong, Z. Peng, and Q. Wang, "Esprit-like two-dimensional direction finding for mixed circular and strictly noncircular sources based on joint diagonalization," *Signal Processing*, vol. 141, pp. 48 – 56, 2017.

[11] H. Chen, C. Hou, W. Liu, W.-P. Zhu, and M. N. S. Swamy, "Efficient two-dimensional direction-of-arrival estimation for a mixture of circular and noncircular sources," *IEEE Sensors Journal*, vol. 16, no. 8, pp. 2527–2536, April 2016.

[12] F. Gao, A. Nallanathan, and Y. Wang, "Improved music under the coexistence of both circular and noncircular sources," *IEEE Transactions on Signal Processing*, vol. 56, no. 7, pp. 3033–3038, July 2008.

[13] A. Liu, G. Liao, Q. Xu, and C. Zeng, "A circularity-based doa estimation method under coexistence of noncircular and circular signals," in *2012 IEEE International Conference on Acoustics, Speech and Signal Processing (ICASSP)*, March 2012, pp. 2561–2564.

[14] X. Wang, L. Wan, M. Huang, C. Shen, and K. Zhang, "Polarization channel estimation for circular and non-circular signals in massive mimo systems," *IEEE Journal of Selected Topics in Signal Processing*, vol. 13, no. 5, pp. 1001–1016, Sep. 2019.

[15] X. Wu, W.-P. Zhu, and J. Yan, "A toeplitz covariance matrix reconstruction approach for direction-of-arrival estimation," *IEEE Transactions on Vehicular Technology*, vol. 66, no. 9, pp. 8223–8237, Sep. 2017.

[16] C. Zhou, Y. Gu, X. Fan, Z. Shi, G. Mao, and Y. D. Zhang, "Direction-of-arrival estimation for coprime array via virtual array interpolation," *IEEE Transactions on Signal Processing*, vol. 66, no. 22, pp. 5956–5971, Nov 2018.

[17] J. Cai, W. Liu, R. Zong, and B. Wu, "Sparse array extension for non-circular signals with subspace and compressive sensing based doa estimation methods," *Signal Processing*, vol. 145, pp. 59 – 67, 2018.

[18] B. N. Bhaskar, G. Tang, and B. Recht, "Atomic norm denoising with applications to line spectral estimation," *IEEE Transactions on Signal Processing*, vol. 61, no. 23, pp. 5987–5999, Dec 2013.

[19] G. Tang, B. N. Bhaskar, P. Shah, and B. Recht, "Compressed sensing off the grid," *IEEE Transactions on Information Theory*, vol. 59, no. 11, pp. 7465–7490, Nov 2013.